ADVANCED FUNCTIONAL MATERIALS
www.afm-journal.de

Direct Growth of Nanocrystalline Graphene/Graphite Transparent Electrodes on Si/SiO$_2$ for Metal-Free Schottky Junction Photodetectors

Zengxing Zhang, Yunxian Guo, Xiaojuan Wang, Dong Li, Fengli Wang, and Sishen Xie**

Conventional methods to produce graphene/silicon Schottky junctions inevitably involve graphene transfer and metal deposition, which leads to the techniques being complicated, high-cost, and environmentally unfriendly. It is possible to directly grow hybrid nanocrystalline graphene/graphite transparent electrodes from photoresist on quartz without any catalyst. Due to the source material being photoresist, nanographene/graphite patterns can easily be made on Si/SiO$_2$ structures to form nanographene/silicon Schottky junctions via commercial photolithography and silicon techniques. The obtained Schottky junctions exhibit excellent properties with respect to photodetection, with photovoltage responsivity of 300 V W^{-1} at a light power of 0.2 μW and photovoltage response time of less than 0.5 s. The devices also exhibit an excellent reliability with the photovoltage deviating less than 1% when cycled over 200 times.

1. Introduction

Graphene, a single atom-thickness carbon layer with a honeycomb structure, has attracted great attention due to its unique structure and fascinating properties.[1–5] Graphene is a 'miracle material' with many superior properties, which give it potential applications in variable fields, including electronics, photonics, composites, and so on.[6] The resistivity of pristine graphene is estimated to be as low as 10^{-6} Ω cm, which is comparable to some metals.[7,8] Furthermore, the absorption of visible light for monolayer graphene is only approximately 2.3%.[9] These properties indicate that graphene could be a promising candidate for transparent electrodes. Based on theoretical calculations, the sheet resistance of monylayer graphene has been predicted to be as low as about 30 Ω □$^{-1}$, which is better than current commercial indium doped tin oxide (ITO) transparent electrodes (typically 30–80 Ω □$^{-1}$ with a transmittance of about 90%).[7,8] Furthermore, compared with ITO, graphene is a metal-free and environmentally friendly material. Therefore, since the discovery of graphene, it has stimulated intense studies on its potential application for transparent electrodes.[10–13]

At the same time, graphene transparent electrodes have been successfully applied for solar cells, light-emitting diodes (LEDs), and photodetectors.[14–17] Silicon, as a prominent semiconducting material, is widely used for commercial photoelectronics. The combination of graphene and silicon for photoelectronics has thus attracted great attention.[18–20] Graphene and silicon can form Schottky junctions. Li et al. reported that graphene/silicon Schottky junctions could be employed as solar cells with the solar energy conversion efficiencies of up to 1.7%.[21] With bis(trifluoromethanesulfonyl)-amide (TFSA) doping in graphene, Miao et al. reported that this energy conversation efficiency can increase up to 8.6%.[22] An et al. reported that graphene/silicon Schottky junctions also show excellent behavior with respect to photodetection, indicating a potential use as ultrasensitive photodetectors.[23] However, further commercial applications of these devices are limited by their fabrication process because the graphene used is often produced by chemical vapor deposition (CVD) or mechanical exfoliation. The former method is often accompanied by a transfer process that results in high cost and complicated techniques, while the latter method is not suitable for large scale. Recently, we developed a catalyst-free method to directly grow nanocrystalline graphene or graphene/graphite patterns on arbitrary substrates from photoresist;[24] this provides a simple and cheap way to fabricate graphene/silicon devices. In this paper, we show that a nanographene/silicon Schottky contact configuration can be easily produced through direct growth of nanocrystalline graphene/graphite transparent electrodes on Si/SiO$_2$ structure by this method, which could provide a practical way to make a variety of metal-free graphene/silicon photoelectronics.

2. Results and Discussion

Nanographene transparent electrodes were obtained with the method that we developed recently.[24] **Figure 1**a shows the

Prof. Z. X. Zhang, Y. X. Guo, Dr. X. J. Wang,
Dr. D. Li, Prof. F. L. Wang
Shanghai Key Laboratory of Special Artificial
Microstructure Materials and Technology
School of Physics Science and Engineering
Tongji University
Shanghai, 200092, China
E-mail: zhangzx@tongji.edu.cn
Prof. S. S. Xie
Beijing National Laboratory for Condensed Matter Physics
Institute of Physics
Chinese Academy of Sciences
Beijing, 100190, China
E-mail: ssxie@iphy.ac.cn

DOI: 10.1002/adfm.201301924

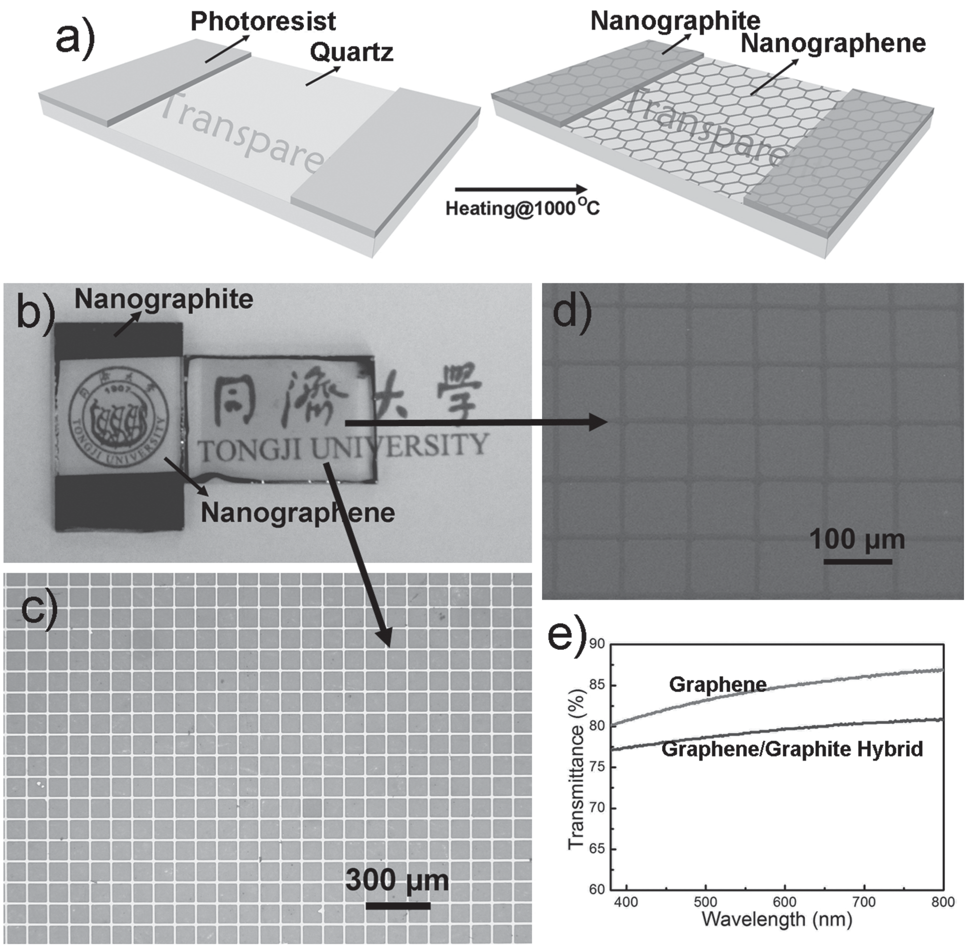

Figure 1. Growth and characterization of hybrid nanocrystalline graphene/graphite transparent electrodes on quartz substrates. a) Schematic growth process of nanocrystalline graphene/graphite on quartz substrates from photoresist. b) Optical photograph of produced transparent electrodes. The central area of the transparent electrode on the left is a few layers nanographene. The transparent electrode on the right is composed of nanographite grids with nanographene filling within the grids. c,d) Optical microscope and SEM images of the indicated transparent electrode. The grid size is 100 µm × 100 µm and the grid line width 10 µm. e) Transmission spectra of the few-layer-thick nanographene and nanographene/graphite hybrid.

growth process schematically. We firstly spin-coated 1.5 µm thick photoresist film on quartz substrates, and then cleaned the central part with an area of around 1 cm × 1 cm by the standard photolithography method. Next, they were heated in a vacuum quartz tube at a temperature of 1000 °C under the protection of 100 SCCM 5% H_2/Ar gas flow. After this process, the preserved photoresist films on the two side parts of quartz were transformed into approximately 150 nm thick nanographite with a few layers of nanographene forming on the central cleaned area. The transformation is due to the aromatic molecules in the photoresist being carbonized and graphitized at high temperature. The formation of the few-layer-thick nanographene on the central part originates from the photoresist molecules being vaporized from the photoresist films and transported onto the central area in the heating process. The left part in Figure 1b shows a typical optical photograph of the obtained nanographene transparent electrode. The two black parts are the nanographite with thickness of around 150 nm; the central part is covered with a few layers of nanographene. We studied the sheet resistance and optical transparency of the produced samples. The sheet resistance of the 150 nm thick nanographite was around 250 $\Omega\ \square^{-1}$ and it was nearly opaque. The few-layer-thick nanographene film on the central area showed a sheet resistance of around 30 $\mathrm{k}\Omega\ \square^{-1}$ and an optical transmittance of around 84.1% at a wavelength of 550 nm (Figure 1e), which is comparable to that of the reported nanographene but several orders of magnitude poorer than that of CVD-derived graphene.[10,25]

In order to improve the conductance of graphene transparent electrodes, several approaches have recently been developed.[11,16,26] Doping graphene can reach a certain sheet resistance, which may be limited by the stability of the graphene–dopant system and increasing cost implications.[27–29] Combining transparent graphene with other opaque structures, such as metal nanowires or grids, is another way to get high-performance graphene-based hybrid transparent electrodes.[8,30] Metal has often been introduced in this approach, and so it is not friendly to the environment. It is well-known that photoresist can be easily and accurately defined into any desired structure by commercial photolithography. We can thus produce

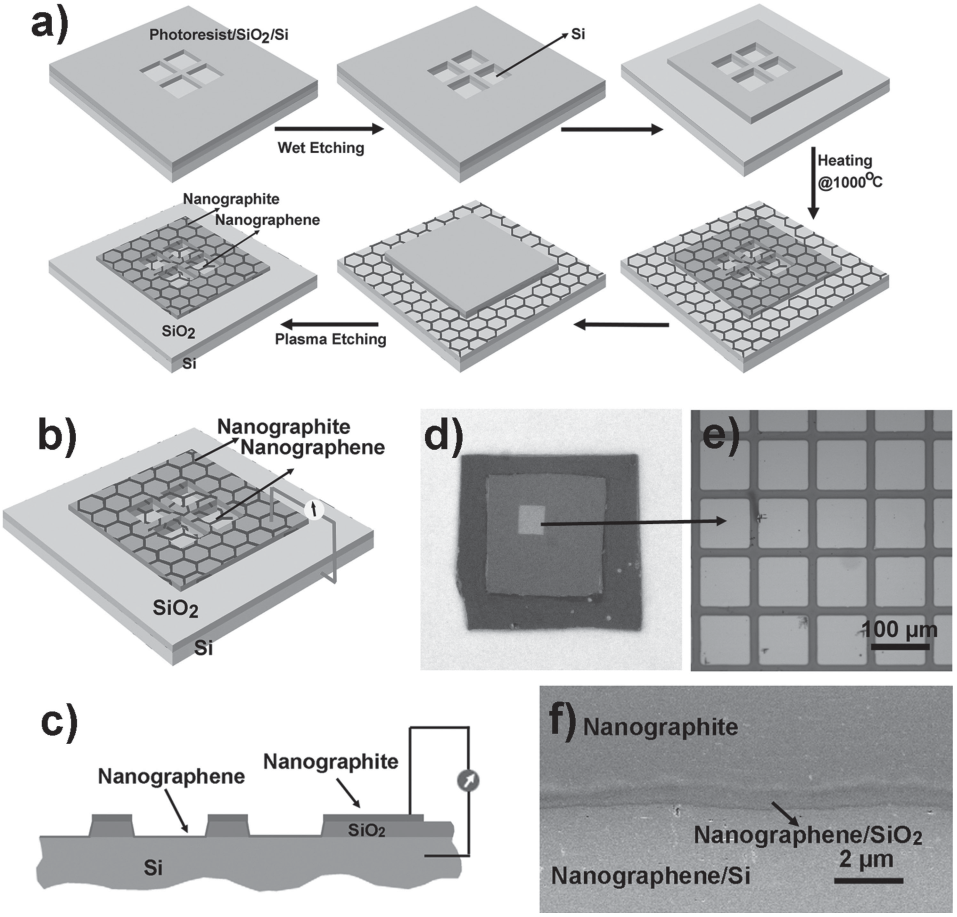

Figure 2. a) Schematic fabrication process of nanographene/graphite-Si/SiO$_2$ configuration. b) Schematic illustration of the top view of the device. c) Schematic illustration of the cross-section view of the device. d) Optical photograph of the obtained device. e) Optical microscope image of the central part indicated. f) SEM image of the tilted top view of the device.

hybrid nanocrystalline graphene/graphite transparent electrodes with the method that we developed.

In this method, we firstly patterned photoresist grids with a grid size of 100 μm × 100 μm and a grid line width of 10 μm on quartz substrates by standard photolithography, and then heated them at a temperature of 1000 °C. The photoresist grids were then transformed into nanographite grids with a few layers of nanographene filling in the area within the grids. The right part in Figure 1b shows a typical optical photograph of the obtained product. Figure 1c and d are the corresponding optical microscopy (OM) and scanning electron microscopy (SEM) images, respectively. The images clearly show that nanographite grids formed on the quartz substrates. The Raman spectra in the Supporting Information further prove that the area within the grids is filled with a few layers of nanographene (Figure S1). The sheet resistance of the obtained hybrid nanocrystalline graphene/graphite grids is approximately 3 kΩ $\square^{-1}$, which is around one order higher than the pure nanographene film with the transparency decreased to around 79.2% at a wavelength of 550 nm (Figure 1e). It should be noted here that the decrease of the transparency is mainly from the nanographite grids, and the few-layer-thick nanographene filling within the grids could have a similar transparency to that of the uniform-thickness nanographene film.

The simple and low-cost fabrication process of the nanographene/graphite transparent electrodes, in addition to the mature technique of photoresist and silicon technology makes them very suitable to design photoelectronics. **Figure 2**a shows the schematic process to fabricate nanographene/graphite transparent electrodes on Si/SiO$_2$ for photodetectors. A 3 mm × 3 mm area of the photoresist grids with the grid size of 100 μm × 100 μm and grid line width of 10 μm was first defined on Si/SiO$_2$ substrates with photoresist film surrounding (see the first step in Figure 2a). Etchant was then used to completely etch the exposed SiO$_2$ area, resulting in the silicon below being exposed. After etching, part of the surrounding photoresist was cleaned so that possible contact between the photoresist and the sides of the substrates could be avoided (see the third step in Figure 2a). After heating, a transparent electrode of nanographene/graphite grids was formed on the substrate with nanographite grids on SiO$_2$ and nanographene on Si and the wall of the etched SiO$_2$. In this way, the nanographite grids and the nanographene are in the aggregate. It should be noted here that a few-layer-thickness of nanographene is also formed on the surrounding cleaned area, which is etched by oxygen plasma in the last step (see Figure 2a). Figure 2d shows a typical optical photograph of the produced devices. In this kind of device, the nanographite around the grids area is employed as electrode to connect the outer electrical circuits so that metal film does not need to be further deposited (a schematic illustration of the device is shown in Figure 2b and c). Figure 2e shows an optical microscope image of the central area of the device, indicating nanographene/graphite grids are formed on the Si/SiO_2 structure (Raman spectra are shown in Figure S2). SEM was also employed to characterize the structure of the obtained devices. Figure 2f shows an SEM image of the tilted top view of the device. The interface between nanographite and SiO_2 or SiO_2 and Si can be clearly observed, exhibiting that there is no direct contact between the nanographite and the etched Si substrate layer.

Typical current–voltage (*I*–*V*) curves of the obtained devices under darkness and light illumination are shown in **Figure 3**a and b, exhibiting conventional rectifying and photodiode-like characteristics. The light source used here was a white light-emitting diode (LED) lamp, the power of which could be modulated up to 5.5 mW cm^{-2}. Under light illumination, the devices exhibit obvious photovoltaic behaviors. The incident light through the nanographene/graphite transparent electrodes generates electron–hole pairs in silicon. These photoexcited carriers are separated by the built-in electrical field in the nanographene/silicon Schottky junction, resulting in the holes being transported from silicon to nanographene and then to the nanographite. Thus, the holes are collected by the nanographene/graphite transparent electrodes and a photovoltage is generated. The open-circuit voltage (V_{OC}) of the device under white light power of 400 µW is around 40 mV (Figure 3a). Further studies indicate that the V_{OC} varied with the power (Figure 3b).

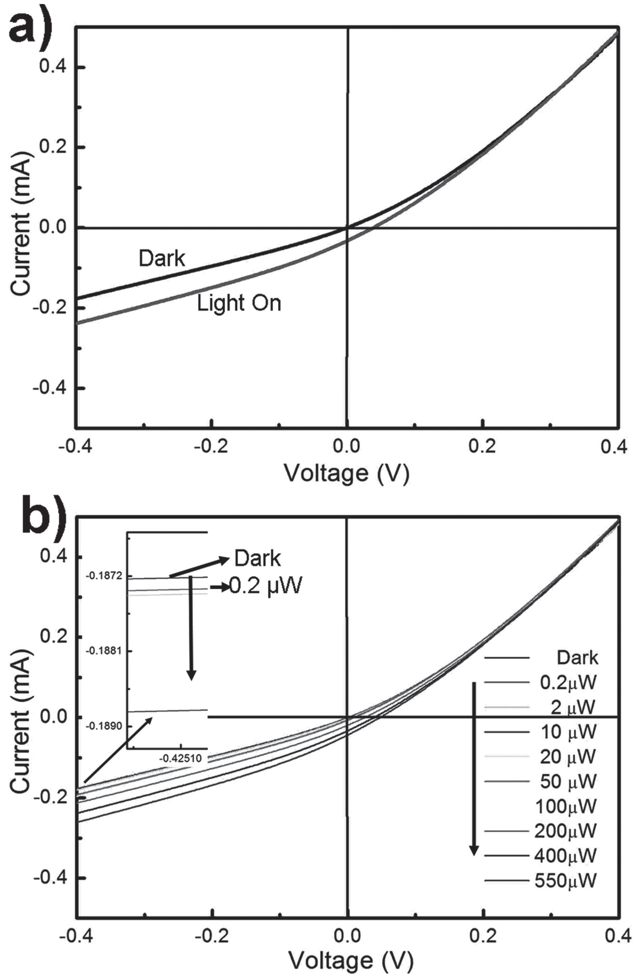

Figure 3. a) *I*–*V* curves of the device under darkness and white light illumination with a power of 400 µW. b) *I*–*V* curves of the device under darkness and white light illumination with different power from 0.2 to 550 µW. The inset is the enlarged image of the indicated part.

The induced photovoltage in the Schottky junction between nanographene and Si can be employed for photodetectors. We tested the devices under a photovoltaic mode. **Figure 4**a shows the photovoltage response of the device to the light with different power for six cycles, clearly indicating that the photovoltage is generated while the light is turned on, and rapidly disappears while the light is turned off. The generated photovoltage increases with the power increasing. Under the light of 2 µW, the photovolatge is about 0.46 mV. While the light power increases to 100 µW, it is about 17 mV. The devices exhibit an excellent photovoltage response to weak signals. We also studied the photovoltage response of the device to white light of 0.2 µW (test limitation). The device shows an obvious photovoltage of approximately 61 µV (see Figure S4 in the Supporting Information). We further studied the photovoltage responsivity of the device at different power; the results are shown in Figure 4b. The photovoltage responsivity R_V (= V_{OC}/P, where V_{OC} is the open-circuit voltage, and P is the incident power) increases rapidly with decreasing light power. Under light of 550 µW, the photovoltage responsivity is around 90 V W^{-1}; when the light decreases to 0.2 µW, the responsivity increases up to around 300 V/W. The dependent relationship of the photovoltage responsivity and the incident power is similar to reported results.[23] It should be noted here that the photovoltage response may be influenced by the thickness of the transparent nanographene. As is well known, the thickness of the nanographene has a deep effect on the optical transmittance and electrical conductivity, which are the critical factors for transparent electrode. Thicker nanographene will decrease the optical transmittance but increase the electrical conductivity. For photodetectors, the former factor would decrease the responsivity but the later might increase it. If the thickness is well optimized, a much higher photovoltage responsivity might be obtained.

Response time is an important characteristic for photodetectors. The fast response time means that the devices can quickly switch from “on” to “off” state or from “off” to “on” state. The nanographene/graphite on Si/SiO_2 configuration gives a fast response time. Figure 4c shows the response times of the photovoltage generation and disappearance corresponding to the light on and off. The power of the light used here is 100 µW. Due to test limitations, we could not exactly obtain the real response time of the devices. The rough measurement indicates that the response time is obviously less than 0.5 s (Figure 4c). Reliability is another important characteristic

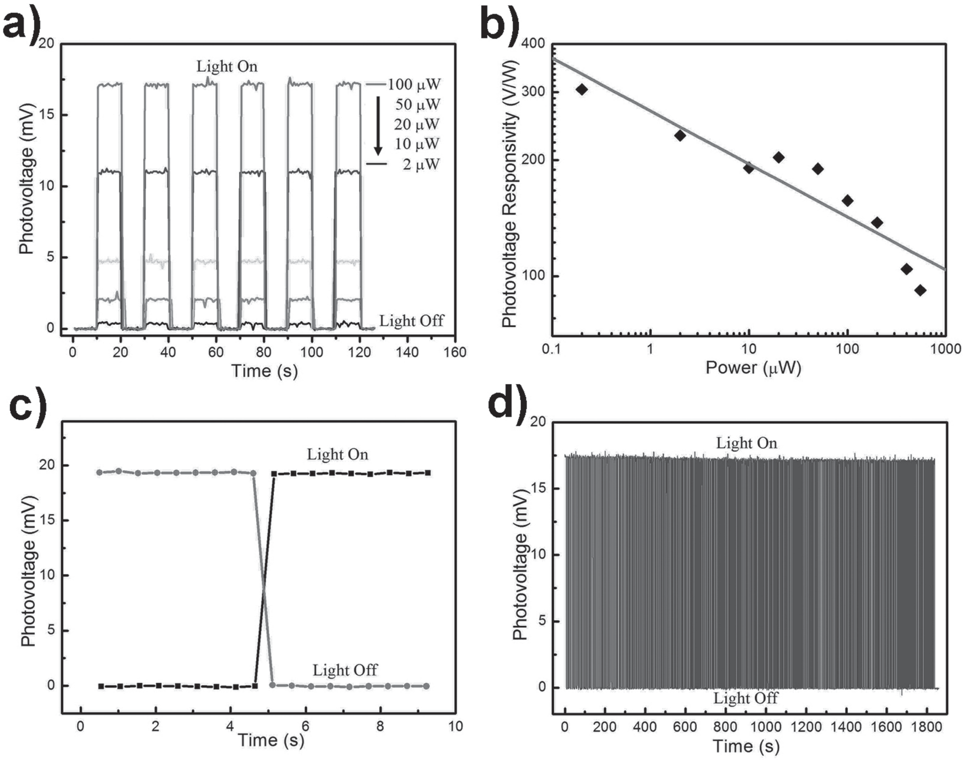

Figure 4. a) Photovoltage response of the device to the light with different power turning on and off; the photovoltage is the open-circuit voltage, V_{OC}. b) Variation of the photovoltage responsivity as a function of incident power. c) Photovoltage response to the light turning on and off; the light was of 100 μW. d) Time-dependent repeatability of switching properties of the device for over 200 cycles.

for photodetectors. Figure 4d shows the photovoltage response curve to the light of 100 μW cycling on and off over 200 times. The deviated photovoltage is less than 1%, thus exhibiting excellent repeatability.

3. Conclusions

A simple and low-cost method to fabricate nanographene/graphite transparent electrodes on Si/SiO_2 structures for Schottky junction configuration has been developed. The devices show excellent photoresponse properties to white light, with a photovoltage responsivity of 300 V W^{-1} at the light power of 0.2 μW and photovoltage response time of less than 0.5 s. The devices also exhibit an excellent reliability, with the deviated photovoltage being less than 1% when repeated for over 200 cycles. Due to the source material being photoresist, it is very easy to achieve device fabrication, integration, and miniaturization; thus, this could be a practical way to make metal-free graphene/silicon photoelectronics for commercial use.

4. Experimental Section

Fabrication of Nanographene/Graphite Structures on Quartz Substrates for Transparent Electrodes: Nanographene/graphite structures on quartz substrates were produced from photoresist with the method that we reported recently.[24] Figure 1a shows the schematic process. In a typical process, the wanted photoresist structures with a thickness of 1.5 μm were patterned on quartz substrates by a standard photolithography method. The photoresist used was RZJ-304 from Suzhou Ruihong Electronic Chemicals Co. Ltd. The samples were then heated for 15 min in a horizontal quartz vacuum tube at 1000 °C under the protection of 100 SCCM 5% H_2/Ar gas flow. After this process, the photoresist structures on quartz substrates were transformed into nanographite with the empty parts being covered with nanographene.

Fabrication of Nanographene/Graphite Grids Structures on Si/SiO₂ for Schottky Junction Photodetectors: The silicon used here was n-type with a resistivity of 1–10 Ω cm, covered with a 300 nm thick thermal oxide film on both sides. Nanographene/graphite structures on Si/SiO_2 were produced as shown schematically in Figure 2a. Firstly, an area of 3 mm × 3 mm of photoresist grids surrounded by a continuous photoresist film was patterned on Si/SiO_2 substrates with the standard photolithography method. The photoresist was 1.5 μm in thickness, the grid size 100 μm × 100 μm, and the grid line width 10 μm. Secondly, the as-obtained photoresist structures on Si/SiO_2 were immersed into etchant solution for wet etching. The etchant was NH_4F/10% HF/H_2O in the ratio 8 g:2 mL:12 mL. Next, the exposed SiO_2 was etched, leaving the silicon underneath with the photoresist-protected SiO_2 parts preserved. Thirdly, the surround part of photoresist was removed to avoid contact between silicon and photoresist. The samples were then heated for 15 min in a horizontal quartz vacuum tube at 1000 °C under the protection of 100 SCCM 5% H_2/Ar gas flow. Next, the photoresist structures on Si/SiO_2 were transformed into nanographite with other parts being covered with a few layers of nanographene. In order to avoid contact between the nanographene and the side silicon, the central structures were protected and the surrounding nanographene was etched by oxygen plasma (the fifth step in Figure 2a).

Transparent Electrode and Schottky Junction Photodetector Characterization: The transmittance of the transparent electrodes was measured with a

Hitachi U-3900H UV-VIS spectrophotometer, and the sheet resistance was measured by the four-probe method. The electrical properties of the devices were characterized in atmosphere at room temperature with a Keithley 4200-SCS semiconductor analyzer. The light source was a white light-emitting diode (LED) lamp whose power can be modulated. We used an optical power meter of SGN-1 to measure the power of the light and calculated the incident light power on the devices according to their area.

Supporting Information

Supporting Information is available from the Wiley Online Library or from the author.

Acknowledgements

The work was supported by the National Science Foundation of China (11104204), the Shanghai Pujiang Program (12PJ1408900), and the Fundamental Research Funds for the Central Universities (1370219139). We thank Dr. Liping Zou for Raman measurements and Prof. Binghui Ge for TEM analysis.

Received: June 5, 2013
Revised: June 27, 2013

---

[1] A. K. Geim, K. S. Novoselov, *Nat. Mater.* **2007**, *6*, 183.
[2] Y. Zhang, Y.-W. Tan, H. L. Stormer, P. Kim, *Nature* **2005**, *438*, 201.
[3] X. L. Li, X. R. Wang, L. Zhang, S. W. Lee, H. J. Dai, *Science* **2008**, *319*, 1229.
[4] H. Zhou, C. Qiu, Z. Liu, H. Yang, L. Hu, J. Liu, H. Yang, C. Gu, L. Sun, *J Am. Chem. Soc.* **2009**, *132*, 944.
[5] L. Ci, L. Song, C. H. Jin, D. Jariwala, D. X. Wu, Y. J. Li, A. Srivastava, Z. F. Wang, K. Storr, L. Balicas, F. Liu, P. M. Ajayan, *Nat. Mater.* **2010**, *9*, 430.
[6] K. S. Novoselov, V. I. Falko, L. Colombo, P. R. Gellert, M. G. Schwab, K. Kim, *Nature* **2012**, *490*, 192.
[7] J.-H. Chen, C. Jang, S. Xiao, M. Ishigami, M. S. Fuhrer, *Nat. Nanotechnol.* **2008**, *3*, 206.
[8] Y. Zhu, Z. Sun, Z. Yan, Z. Jin, J. M. Tour, *ACS Nano* **2011**, *5*, 6472.
[9] R. R. Nair, P. Blake, A. N. Grigorenko, K. S. Novoselov, T. J. Booth, T. Stauber, N. M. R. Peres, A. K. Geim, *Science* **2008**, *320*, 1308.
[10] X. Li, Y. Zhu, W. Cai, M. Borysiak, B. Han, D. Chen, R. D. Piner, L. Colombo, R. S. Ruoff, *Nano Lett.* **2009**, *9*, 4359.
[11] H. Chang, G. Wang, A. Yang, X. Tao, X. Liu, Y. Shen, Z. Zheng, *Adv. Funct. Mater.* **2010**, *20*, 2893.
[12] J. K. Wassei, R. B. Kaner, *Mater. Today* **2010**, *13*, 52.
[13] K. S. Kim, Y. Zhao, H. Jang, S. Y. Lee, J. M. Kim, K. S. Kim, J.-H. Ahn, P. Kim, J.-Y. Choi, B. H. Hong, *Nature* **2009**, *457*, 706.
[14] X. Wang, L. Zhi, K. Mullen, *Nano Lett.* **2007**, *8*, 323.
[15] C.-L. Hsu, C.-T. Lin, J.-H. Huang, C.-W. Chu, K.-H. Wei, L.-J. Li, *ACS Nano* **2012**, *6*, 5031.
[16] V. C. Tung, L.-M. Chen, M. J. Allen, J. K. Wassei, K. Nelson, R. B. Kaner, Y. Yang, *Nano Lett.* **2009**, *9*, 1949.
[17] Z. Liu, Q. Liu, Y. Huang, Y. Ma, S. Yin, X. Zhang, W. Sun, Y. Chen, *Adv. Mater.* **2008**, *20*, 3924.
[18] C.-C. Chen, M. Aykol, C.-C. Chang, A. F. J. Levi, S. B. Cronin, *Nano Lett.* **2011**, *11*, 1863.
[19] T. Feng, D. Xie, Y. Lin, Y. Zang, T. Ren, R. Song, H. Zhao, H. Tian, X. Li, H. Zhu, L. Liu, *Appl. Phys. Lett.* **2011**, *99*, 233505.
[20] C. Xie, P. Lv, B. Nie, J. Jie, X. Zhang, Z. Wang, P. Jiang, Z. Hu, L. Luo, Z. Zhu, L. Wang, C. Wu, *Appl. Phys. Lett.* **2011**, *99*, 133113.
[21] X. Li, H. Zhu, K. Wang, A. Cao, J. Wei, C. Li, Y. Jia, Z. Li, X. Li, D. Wu, *Adv. Mater.* **2010**, *22*, 2743.
[22] X. Miao, S. Tongay, M. K. Petterson, K. Berke, A. G. Rinzler, B. R. Appleton, A. F. Hebard, *Nano Lett.* **2012**, *12*, 2745.
[23] X. An, F. Liu, Y. J. Jung, S. Kar, *Nano Lett.* **2013**, *13*, 909.
[24] Z. Zhang, B. Ge, Y. Guo, D. Tang, X. Wang, F. Wang, *Chem. Commun.* **2013**, *49*, 2789.
[25] H. Medina, Y.-C. Lin, C. Jin, C.-C. Lu, C.-H. Yeh, K.-P. Huang, K. Suenaga, J. Robertson, P.-W. Chiu, *Adv. Funct. Mater.* **2012**, *22*, 2123.
[26] D.-W. Wang, F. Li, J. Zhao, W. Ren, Z.-G. Chen, J. Tan, Z.-S. Wu, I. Gentle, G. Q. Lu, H.-M. Cheng, *ACS Nano* **2009**, *3*, 1745.
[27] P. Blake, P. D. Brimicombe, R. R. Nair, T. J. Booth, D. Jiang, F. Schedin, L. A. Ponomarenko, S. V. Morozov, H. F. Gleeson, E. W. Hill, A. K. Geim, K. S. Novoselov, *Nano Lett.* **2008**, *8*, 1704.
[28] S. Bae, H. Kim, Y. Lee, X. Xu, J.-S. Park, Y. Zheng, J. Balakrishnan, T. Lei, H. Ri Kim, Y. I. Song, Y.-J. Kim, K. S. Kim, B. Ozyilmaz, J.-H. Ahn, B. H. Hong, S. Iijima, *Nat. Nanotechnol.* **2010**, *5*, 574.
[29] K. K. Kim, A. Reina, Y. Shi, H. Park, L.-J. Li, Y. H. Lee, J. Kong, *Nanotechnology* **2010**, *21*, 285205.
[30] J.-Y. Lee, S. T. Connor, Y. Cui, P. Peumans, *Nano Lett.* **2008**, *8*, 689.